Supplementary Information

Intrinsic Quantum Anomalous Hall Effect in TaPdXTe (X = S, Se) monolayer

Haofeng Wei [a], Yanzhao Wu[a], Junwei Tong[b], Li Deng[a], Xiang Yin[a], Zhijun Zhang[c], and Xianmin Zhang[a]*

[a]Key Laboratory for Anisotropy and Texture of Materials (Ministry of Education), School of Material Science and Engineering, Northeastern University, Shenyang, 110819, China

[b]Department of Physics, Freie Universität Berlin, Berlin, 14195, Germany

[c]Liaoning Institute of Science and Technology, Benxi 117004, China

In this study, the first-principles calculations based on Density Functional Theory (DFT) are performed using the Vienna ab initio simulation package (VASP)[1, 2]. The interaction between electrons and ions is described using the projector-augmented wave (PAW) method[3, 4]. The generalized gradient approximation (GGA) with the Perdew-Burke-Ernzerhof (PBE) formalism is used to describe the exchange-correlation interaction[5]. A 11 × 11 × 1 Monkhorst-Pack k-point meshes is used to sample the Brillouin zone[6]. The cut-off energy is set to 500 eV. The convergence criteria for force and energy are 0.005 eV/Å and 10^{-8} eV, respectively. The vacuum layer in the z direction is set to 15 Å, thus avoiding interactions between neighboring layer atoms. The d orbitals of Ta and Pd atoms are treated using the PBE+U_{eff} method[7], with the Hubbard U_{eff} parameter set to 4 eV[8]. Phonon spectrum is calculated using a 3 × 3 × 1 supercell and the PHONOPY package[9, 10]. Ab initio molecular dynamics simulations are performed under the NVT ensemble at 300 K[11]. The data for the calculations are processed using the VASPKIT package[12]. A maximized localization function is created using the WANNIER90 package[13]. The Berry curvature, anomalous Hall conductivity, and chiral edge state are calculated using the WannierTools package[14]. The T_C is calculated through Monte Carlo (MC) simulations, and MC simulations are performed using a 32 × 32 × 1 supercell and 1 × 10^7 steps at each temperature.

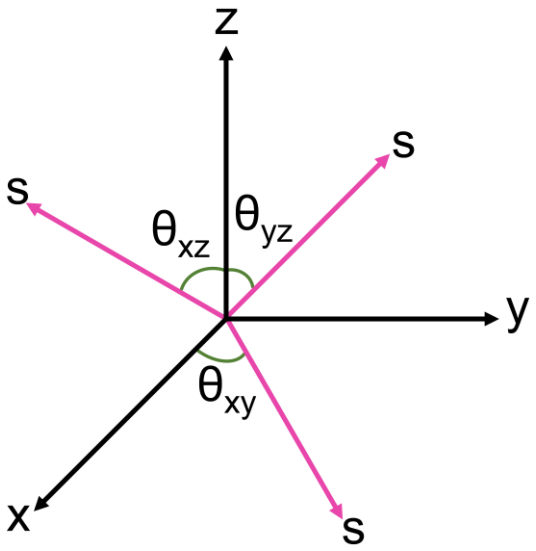

Fig. S1. The Schematic diagram shows the spin vector S rotating at an angle θ from 0 to 180° in xy, xz, and yz planes.

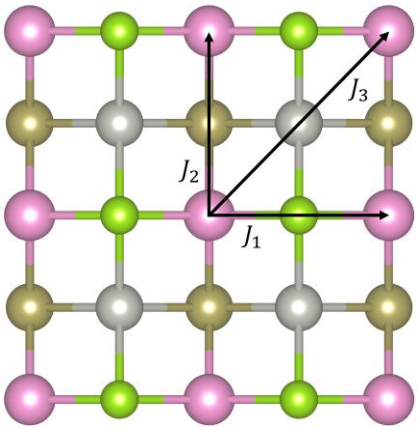

Fig. S2. Schematic diagram of the three exchange parameters (J_1, J_2, and J_3) for TaPdSTe (TaPdSeTe) monolayer.

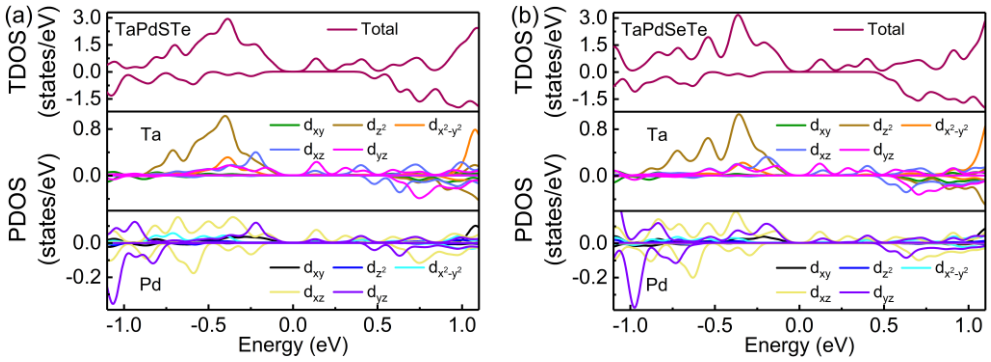

Fig. S3. Total density of states (TDOS) and projected density of states (PDOS) for the Ta and Pd atoms of (a) TaPdSTe and (b) TaPdSeTe monolayers.

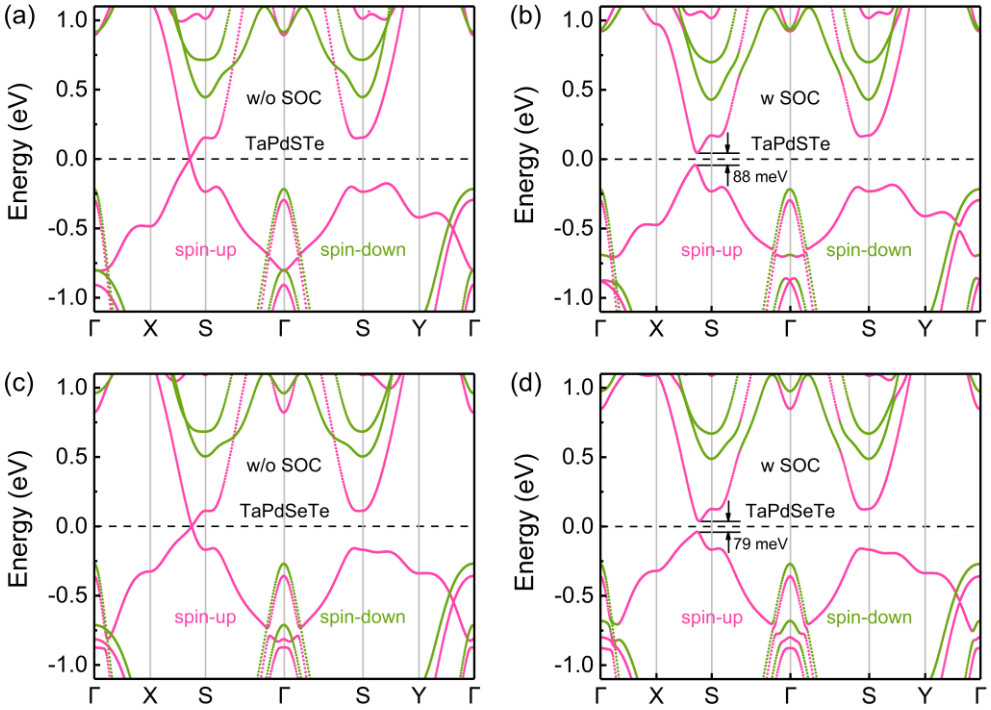

Fig. S4. The spin-resolved energy bands for TaPdSTe monolayer (a) without SOC and (b) with SOC effect. The spin-resolved energy bands for TaPdSeTe monolayer (c) without SOC and (d) with SOC effect.

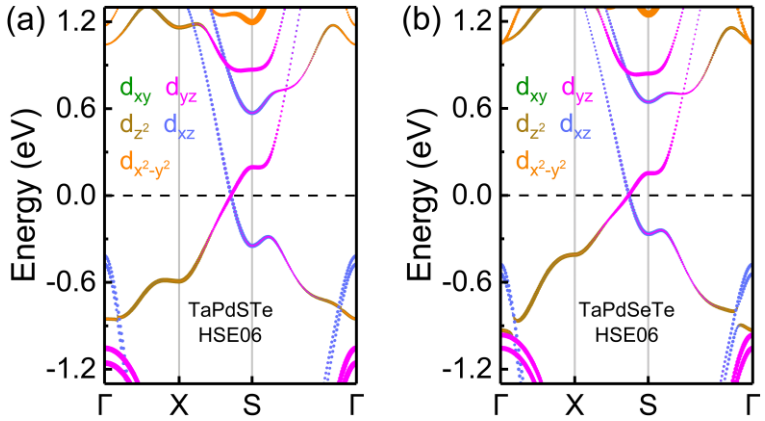

Fig. S5. (a) Orbit-resolved energy bands for TaPdSTe monolayer without considering SOC effect from HSE06 method. (b) Orbit-resolved energy bands for TaPdSeTe monolayer without considering SOC effect from HSE06 method.

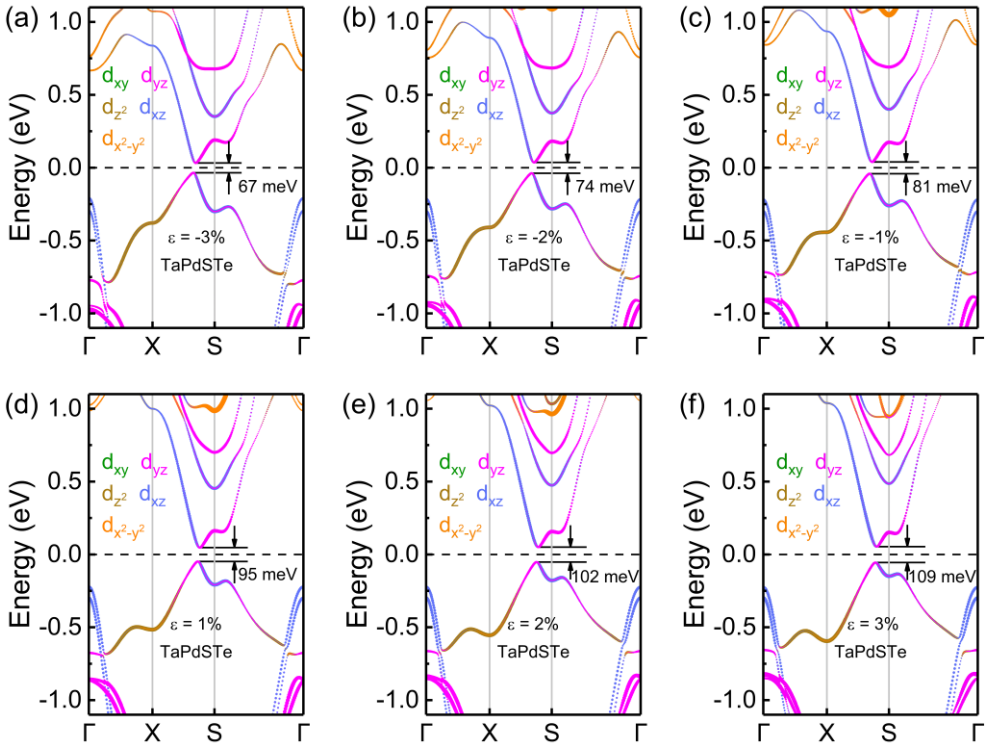

Fig. S6. Orbit-resolved energy bands for TaPdSTe monolayer with SOC effect under (a) -3%, (b) -2%, (c) -1%, (d) 1%, (e) 2%, and (f) 3% strains.

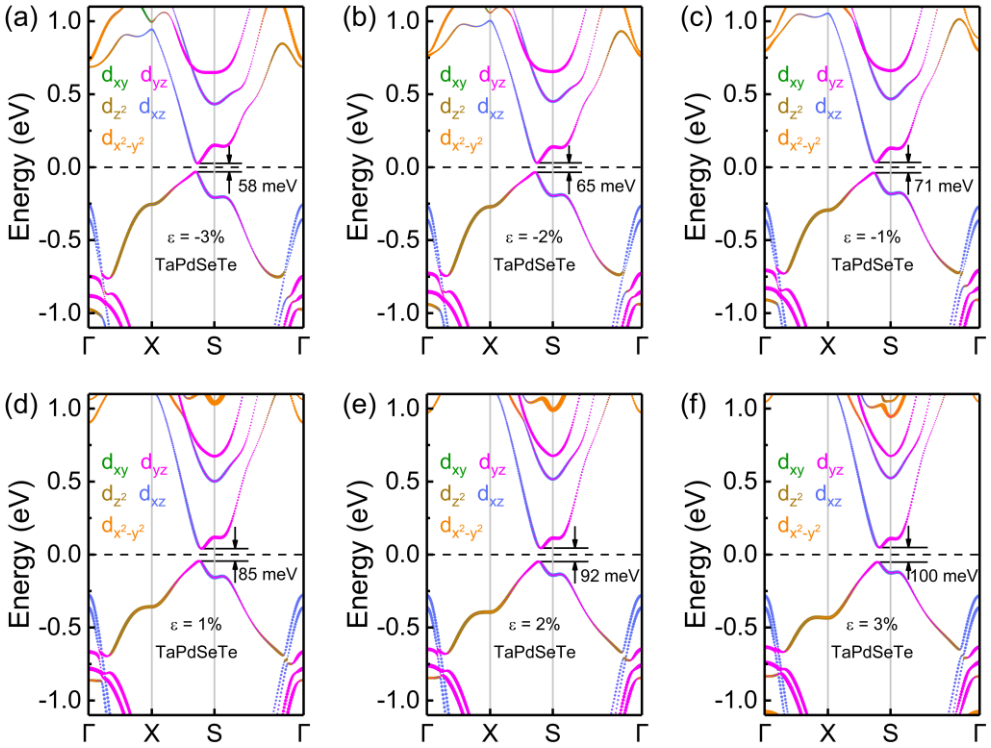

Fig. S7. Orbit-resolved energy bands for TaPdSeTe monolayer with SOC effect under (a) -3%, (b) -2%, (c) -1%, (d) 1%, (e) 2%, and (f) 3% strains.

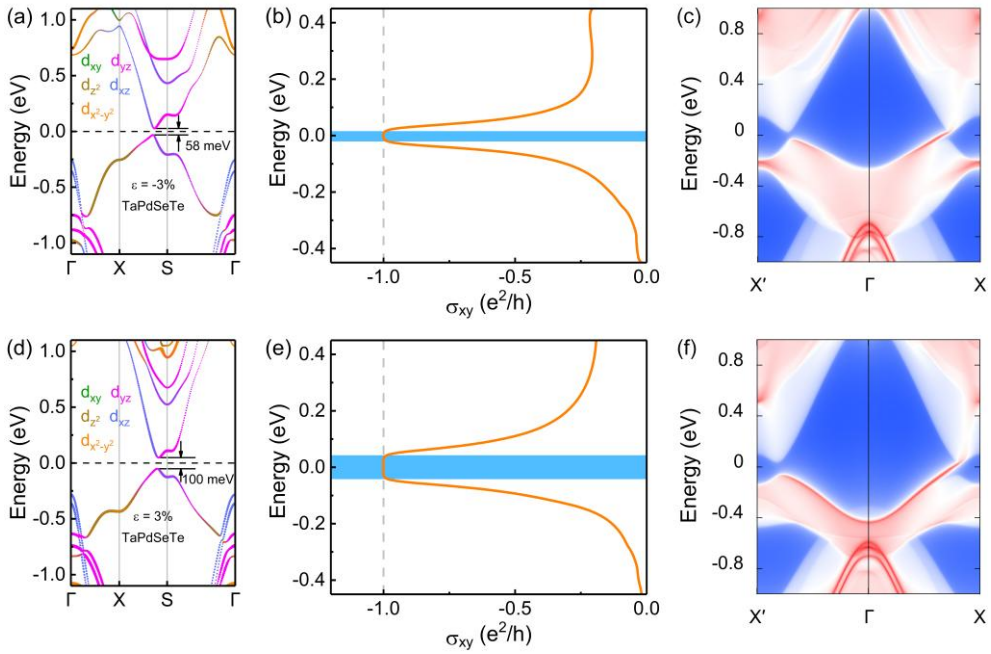

Fig. S8. (a) Orbit-resolved energy bands with SOC effect, (b) AHC, and (c) chiral edge state for TaPdSeTe monolayer under -3% strain. (d) Orbit-resolved energy bands with SOC effect, (e) AHC, and (f) chiral edge state for TaPdSeTe monolayer under 3% strain.

References

[1] Kresse, G.; Furthmüller, J. Efficiency of ab-initio total energy calculations for metals and semiconductors using a plane-wave basis set. Computational Materials Science, 1996, 6, 15-50.

[2] Kresse, G.; Furthmüller, J. Efficient iterative schemes for ab initio total-energy calculations using a plane-wave basis set. Physical Review B, 1996, 54, 11169-11186.

[3] Blöchl, P. E. Projector augmented-wave method. Physical Review B, 1994, 50, 17953-17979.

[4] Kresse, G.; Joubert, D. From Ultrasoft pseudopotentials to the projector augmented-wave method. Physical Review B, 1999, 59, 1758-1775.

[5] Perdew, J. P.; Burke, K.; Ernzerhof, M. Generalized gradient approximation made simple. Physical Review Letters, 1996, 77, 3865-3868.

[6] Monkhorst, H. J.; Pack, J. D. Special points for Brillouin-zone integrations. Physical Review B, 1976, 13, 5188-5192.

[7] Aryasetiawan, F.; Karlsson, K.; Jepsen, O.; Schönberger, U. Calculations of Hubbard U from first-principles. Physical Review B, 2006, 74, 125106.

[8] He, S.; Kang, R.; Zhou, P.; Lyu, P.; Sun, L. Excellent intrinsic Chern insulators: monolayer $PdTaX_2$ (X = Se, Te). Journal of Materials Chemistry C, 2024, 12, 4062-4069.

[9] Baroni, S.; de Gironcoli, S.; Dal Corso, A.; Giannozzi, P. Phonons and related crystal properties from density-functional perturbation Theory. Reviews of Modern Physics, 2001, 73, 515-562.

[10] Togo, A.; Tanaka, I. First principles phonon calculations in materials science. Scripta Materialia, 2015, 108, 1-5.

[11] Martyna, G. J.; Klein, M. L.; Tuckerman, M. Nosé-Hoover chains: The canonical ensemble via continuous dynamics. The Journal of Chemical Physics, 1992, 97, 2635-2643.

[12] Wang, V.; Xu, N.; Liu, J.-C.; Tang, G.; Geng, W.-T. VASPKIT: a user-friendly interface facilitating high-throughput computing and analysis using VASP code. Computer Physics Communications, 2021, 267, 108033.

[13] Mostofi, A. A.; Yates, J. R.; Lee, Y.-S.; Souza, I.; Vanderbilt, D.; Marzari, N. wannier90: a tool for obtaining maximally-localised wannier functions. Computer Physics Communications, 2008, 178, 685-699.

[14] Wu, Q.; Zhang, S.; Song, H.-F.; Troyer, M.; Soluyanov, A. A. WannierTools: an open-source software package for novel topological materials. Computer Physics Communications, 2018, 224, 405-416.